Validation of On-board Cloud Cover Assessment Using EO-1

Dan Mandl
Code 584
NASA/GSFC
Greenbelt, Md. 20771
301-286-4323
Daniel.J.Mandl@Nasa.gov

Michael Griffin and Hsiao-hua Burke
S4-257 Group 97
MIT Lincoln Laboratory
Lexington, MA. 02420-9185
(781)981-0396
griffin@ll.mit.edu

Jerry Miller
Code 586
NASA/GSFC
Greenbelt, Md. 20771
(301)286-5823
Jerome.Miller-1@nasa.gov

Abstract— **The purpose of this NASA Earth Science Technology Office funded effort was to flight validate an on-board cloud detection algorithm and to determine the performance that can be achieved with a Mongoose V flight computer. This validation was performed on the EO-1 satellite, which is operational, by uploading new flight code to perform the cloud detection. The algorithm was developed by MIT/Lincoln Lab and is based on the use of the Hyperion hyperspectral instrument using selected spectral bands from 0.4 to 2.5 µm. The Technology Readiness Level (TRL) of this technology at the beginning of the task was level 5 and was TRL 6 upon completion.**

In the final validation, an 8 second (0.75 Gbytes) Hyperion image was processed on-board and assessed for percentage cloud cover within 30 minutes. It was expected to take many hours and perhaps a day considering that the Mongoose V is only a 6-8 MIP machine in performance. To accomplish this test, the image taken had to have level 0 and level 1 processing performed on-board before the cloud algorithm was applied. For almost all of the ground test cases and all of the flight cases, the cloud assessment was within 5% of the correct value and in most cases within 1-2%.

Keywords: hyperspectral, cloud cover, EO-1, Hyperion

TABLE OF CONTENTS

1. INTRODUCTION

On-board cloud cover assessment has the potential to considerably reduce the resources on downlink for unwanted scenes. The problem thus far has been the performance of existing on-board computers. This validation was an experiment on what could be accomplished using the Mongoose V which at the time of the validation was one of the fastest flight computers that was flying for NASA. EO-1 had completed it's prime mission and it also had two on-board Mongoose V computers, each with 256 Mbytes of memory and thus presented an opportunity to perform an on-orbit test of this technology.

The New Millennium Program's first Earth-observing mission (EO-1) is a technology validation mission. It is managed by the NASA Goddard Space Flight Center in Greenbelt, Maryland and launched in November 2000. The purpose of this mission was to flight-validate revolutionary technologies that will contribute to the reduction of cost and increase of capabilities for future land imaging missions. For the prime mission, there were five instrument, five spacecraft, and three supporting technologies to flight-validate during a year of operations. Following the first year of operations, the EO-1 mission entered its extended mission phase in which additional validations were performed on the existing on-board technologies and new technologies such as this on-board cloud covered assessment that had not originally been planned for the mission.

There were many challenges to accomplishing this validation experiment. For example, to perform an on-board cloud cover assessment, first an image needed to have level 0 and level 1 processing performed before the cloud assessment algorithm could be applied. In order to accomplish this task, the Flight Software developers in conjunction with MIT/Lincoln Lab (MIT/LL) had to develop more than one Mbyte of code, test the code on the flight software testbed and uplink that code through a 2 kbps uplink. It took days to upload the code for just one attempt. The general approach, additional challenges and results of this task are described in the following sections.

2. SKILL MIX

In order to accomplish this validation, a diverse set of skills was needed. The skill sets included expertise in mission systems engineering, remote sensing with hyperspectral instrumentation, operations engineering, flight software development for EO-1 and ground system engineering . The team consisted of 17 people from GSFC, MIT/LL, Microtel-LLC, Honeywell, CSC, Compaq and Mitretek. The complete list of participants is in the final section.

decisions whether to dispose of an image before downlinking due to obstruction of a desired image of the ground via clouds.   The algorithm was designed to discriminate between clouds, snow, ice, sand and other types of ground cover.

More importantly, the final validation demonstrated that by creatively designing the on-board algorithms, even with today's slow flight computers such as the Mongoose V, cloud assessment could occur within 30 minutes.   This result surprised the team. Our original estimate was that it would take hours if not days to complete one cloud

Figure 1- Left two panels are scan lines 1700-2700 of a Hyperion image collected over Kauai, HI along with the cloud mask, displaying cloudy conditions with cumulus clouds over land and water. The scene was taken on May 22, 2002 at 2056 UTC. The algorithm computed the cloud amount for the scene to be 41.3%.

3. RESULTS

Twenty Hyperion images were selected from the archive to help test the algorithm on the ground before flight. Figure 1 shows a portion of one of the images used along with the derived cloud mask that the algorithm generated. Figure 3 shows the final validation image of El Mhamid which was assessed for cloud cover and derived a cloud score of 43%. The results of the algorithm were validated on the ground by manually running the algorithm on a few scan lines, generating a cloud mask and comparing the flight generated results with the ground results. The scan lines were visually inspected to determine if the pixels were cloud covered or not. The onboard validation discriminated clouds within 1-2% which met our criteria of 5%.   It was felt that 5% accuracy was sufficient to allow subsequent on-board

assessment on-board EO-1.   Furthermore, the team determined that faster results could be derived without much loss of precision by three methods, two of which we could do on EO-1 in the future and one relegated to an improved design of the flight computer n the future. First, we could sub-sample the pixels at a rate of 1:5 and approximate closely the same results. We could also only processes a portion of the image representing the area of interest.   Using these techniques, we estimated that the cloud assessment of one Hyperion image (.75 Gbytes) could be reduced to under 5 minutes! The final method to speed up the onboard cloud assessment process would be if we had direct access to the science recorder and we processed the data in the Science recorder memory rather than moving the image over to the Mongoose V memory.
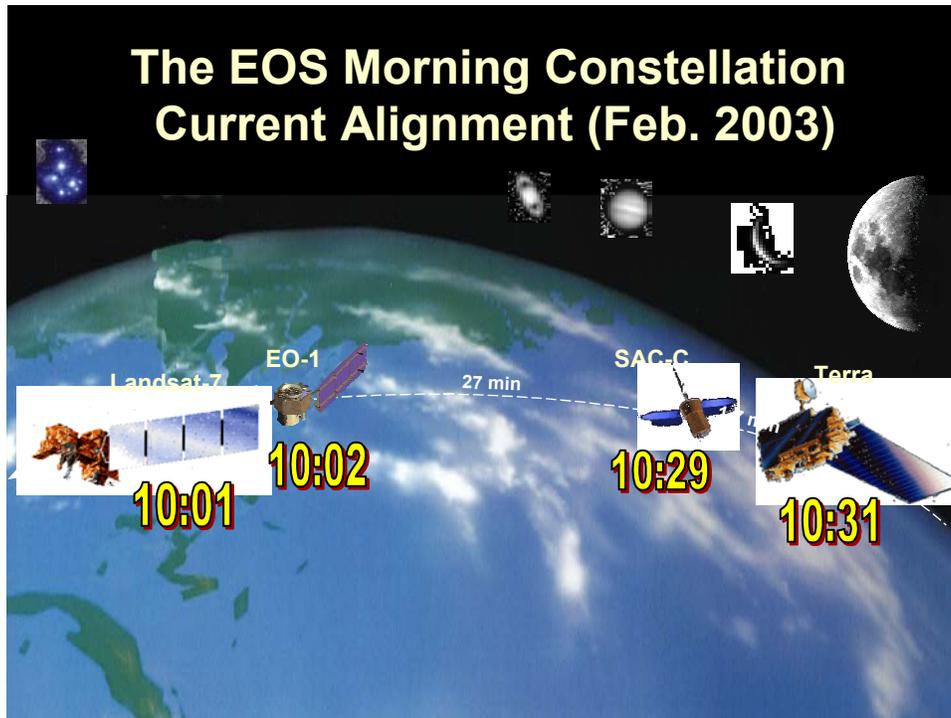
Figure 2 – EO-1 Mission Pictorial showing formation flying with Landsat, SAC-C and Terra

4. EO-1 MISSION AND SPACECRAFT OVERVIEW

EO-1 flies in the Earth Observing System (EOS) "Morning Constellation". It is about one minute behind Landsat and about 30 minutes ahead of SAC-C and Terra. EO-1 is at a 705 km altitude, a 98.7 degree inclination and a 16 day repeat track.

There are two Mongoose V processors onboard, one to control the Command and Data Handling (C&DH) and the .other to control the Wideband Advanced Recorder Precessor (WARP) science recorder. Each Mongoose is 12 Mhz and runs at about 6-9 MIPS supported by 256 Mbytes of memory. They both run on VxWorks 5.3.1. The WARP Mongoose is unused except during image collection and occasional S-Band downlink events.

Figure 4 shows the WARP Mongoose flight software architecture. The architecture consists of a software bus on top of a VxWorks operating systems. For this task, the Memory Dwell task was used to host the cloud cover assessment software.

Figure 3   Portion of Hyperion image, El Mhamid, which was the final validation image taken on-board March 4, 2003.
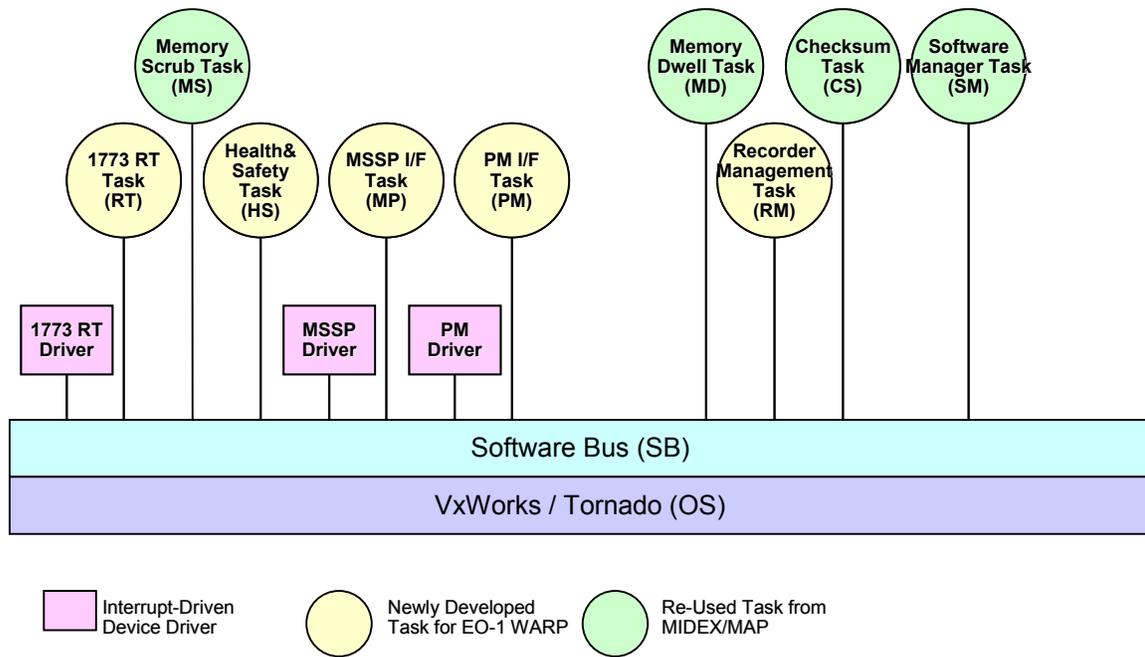
Figure 4 – EO-1 Existing WARP Mongoose Flight Software Architecture

5. CLOUD ASSESSMENT SOFTWARE & ALGORITHM

The software that was developed had to perform the following functionality:

- Perform playback of image data files stored in WARP into the WARP Mongoose memory
- Extract pixel readout level 0 values from bands used by algorithm (0.55, 0.66, 0.86, 1.25, 1.38 and 1.65 μm)
- Apply level 1 calibration to each level 0 data sample
- Perform pixel-by-pixel testing using reflectance data to determine which pixels are cloud covered
- Cloud coverage for a given pixel determined by a series of tests which include reflectance tests, ratio tests, Normalized Snow Index (NDSI) tests and combined tests
- Statistics provided to count total pixels tested and total pixels cloudy

Figure 5 shows the Hyperion bands that are used in the cloud algorithm and what each band discriminates.

The Hyperion Cloud Cover (HCC) algorithm utilizes six Hyperion bands to discriminate all types of clouds from other surface features in a scene. The selection of the six bands provided spectral information at critical wavelengths while keeping processing costs to a minimum. This was a key aspect of the entire cloud cover detection process, since

Band (μm)	Usage
0.55	Snow/ice/cloud test
0.66	Red reflectance test Vegetation ratio test
0.86	Vegetation ratio test Desert/sand test
1.25	Snow/ice/cloud test Desert/sand test
1.38	High cloud test Ice/low cloud test
1.65	Snow/ice/cloud test Desert/sand test

Figure 5 – Hyperion bands used in cloud assessment algorithm

both onboard computer memory and processing time were limited. The six bands chosen for the initial form of the HCC include two visible channels (0.55 and 0.66 μm), a near-IR channel (0.86 μm) and three SWIR channels (1.25, 1.38 and 1.65 μm). Utilizing these six channels, formulas have been adapted or developed relating the spectral

measurements to discriminate and identify cloud features in a scene. Fig. 6 provides a flowchart of the HCC algorithm. A brief description of the phenomenology behind the algorithm follows. Each test detailed below is designed to eliminate specific non-cloud features.

A. Conversion of radiance to reflectance

Channels with center wavelengths up to 3 μm derive their signal primarily from reflected solar energy off land, water and cloud features. The reflectivity of an object in a scene is generally not a function of the incident solar insolation (although it is a function of the viewing geometry). Therefore, deriving the reflectance for a scene removes the variation in the solar illumination with wavelength.

For the Hyperion sensor, where reflected solar flux is the primary illumination source, it is useful to convert the channel radiance L_i to an *at-sensor* reflectance ρ_i. This can be accomplished by dividing the channel radiance by the incident solar flux $F_{0,i}$ corrected for sun angle μ_0 and earth-sun distance d_{e-s} (in *Astronomical Units, AU*),

$$\rho_i = \left(\frac{\pi}{\mu_0 F_{0,i} / d_{e-s}^2} \right) L_i \quad .$$

The sun angle is defined by $\mu_0 = \cos(\theta_0)$, where θ_0 is the solar zenith angle. For this implementation, θ_0 is provided through the EO-1 telemetry. The earth-sun distance is a function of the Julian day and is computed using a parameterized function of the actual earth-sun distance variation. The incident solar flux as a function of wavelength $F_0(\lambda)$ can be obtained from a number of sources; the MODTRAN radiative transfer model [3] contains a solar illumination database which can be convolved with the band spectral response functions to obtain the channel solar flux F_{0i}.

B. High clouds

High clouds typically have spectral reflectance characteristics that are similar to other cloud types. However, high thin predominantly ice clouds are generally not opaque to underlying surface reflectance, such that surface features can be observed through the clouds. Techniques using observations in the water vapor absorption bands have provided a new method to discriminate high clouds from low clouds and surface features [4][5]. At this wavelength the water vapor absorption is typically strong enough to suppress the contribution from both the reflectance from the surface and low-altitude clouds while adequately transmitting radiation scattered from high-altitude clouds. However, in polar latitudes or at high elevations, the amount of moisture in the atmosphere is greatly reduced, resulting in reduced water vapor absorption in the 1.38 μm band. This increases the penetration of observations at these wavelengths and increases the possibility of some significant surface reflectance contribution to the signal. In these cases, bright surface features (snow or ice) may be mistaken for high clouds. Further testing is required to discriminate these
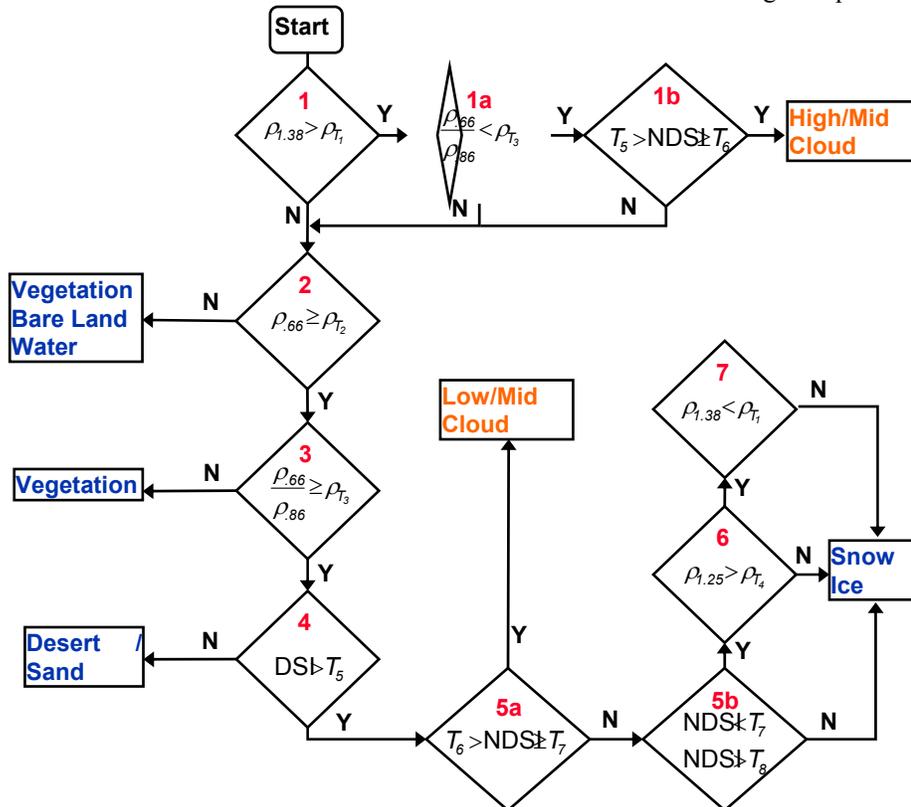
Figure 6. Flowchart of the cloud cover detection process.

features. All pixels that are not flagged as high clouds are passed on for further testing.

C. Reflectance at 0.66 μm

Clouds are typically one of the brightest features in a Hyperion image. The reflectance from clouds is nearly invariant in the visible and near-IR window regions, since the size of the scatterers in the cloud are much larger (size parameter >> 1) than the sensor wavelengths. In the visible spectral band, dark surface objects can be distinguished from bright clouds by a simple reflectance threshold test. At 0.66 μm, many surface features such as water, vegetation, shadowed areas and soil exhibit low reflectance values (< 0.15) and can be easily flagged.

D. Vegetation index ratio

Vegetated surfaces exhibit a strong reflectance gradient near 0.7 μm, known as the red edge [6]. The reflectance for vegetation changes from ~ 0.1 in the visible to 0.4 or greater in the NIR depending on specific aspects of the vegetation cover (health, greenness, etc.). Clouds on the other hand display a nearly constant reflectance signal over this range. Therefore, a ratio of a visible to a NIR channel should be close to 1 for clouds and less than 0.5 for vegetated surfaces. Snow and ice surfaces have a similar behavior to clouds in this spectral region. Fig. 7 provides an example of Hyperion reflectance values for clouds, vegetation and surface ice where the previously mentioned relationships can be observed.
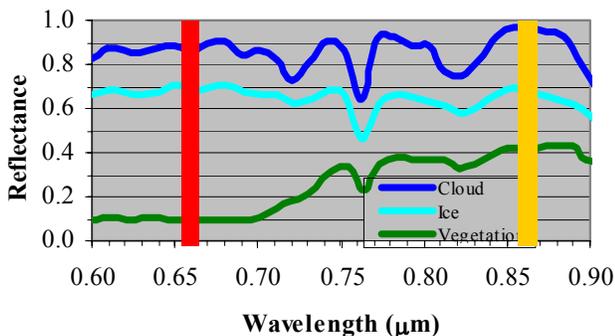
Figure 7 Example of Hyperion reflectance values for clouds

E. Desert sand index

Bright surface features such as snow, ice and sand can easily be mistaken for cloud features in the visible portion of the spectrum. In contrast to other bright surface features such as snow and ice, desert sand tends to display the largest reflectance near 1.6 mm whereas clouds, snow and ice show peaks in the visible and NIR. These observations provide an empirical means to formulate a discrimination index, or Desert Sand Index (DSI) as shown in the formula below,

$$DSI = \frac{\rho_{0.86} - \rho_{1.65}}{\rho_{0.86} + \rho_{1.65}}.$$

In Fig. 8, plots of the Hyperion-observed spectral reflectance for snow, ice, desert and cloud features are shown. Comparing values near the red and orange vertical bands shows that the sand feature is the only one that will display a negative DSI value.

F. Normalized snow index

The Normalized Difference Snow Index (NDSI) is used to identify snow and ice covered surfaces and for separating snow/ice and cumulus clouds. The NDSI measures the relative difference between the spectral reflectance in the visible and SWIR. The technique is analogous to the normalized-difference vegetation index (NDVI), which provides a measure of the health and greenness of vegetated surfaces. The formula commonly used for the NDSI is given by [6],

NDSI values greater than approximately 0.4 are representative of various snow-covered conditions with pure snow having the highest NDSI values. The NDSI tends to decrease as other features (such as soil and vegetation) are mixed in with the snow.
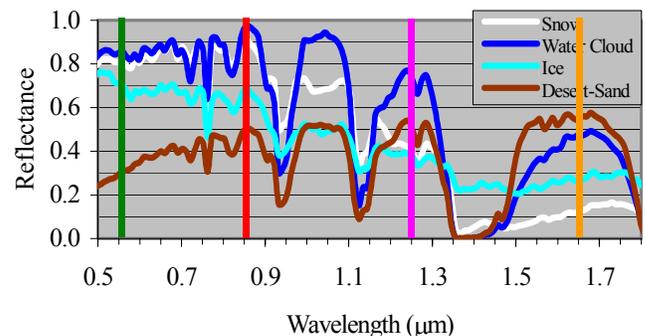
Figure 8. Plot of the spectral signatures for four features in the visible, NIR and SWIR.

G. Reflectance at 1.25 μm

Some moderately bright surface features (such as aged or shadowed snow) may fail the NDSI test. Many of these features can be eliminated from consideration as cloud by comparing their reflectance at 1.25 μm to an empirically defined threshold. Most surface features have reflectance values less than 0.4 at this wavelength while clouds still display reflectances greater than 0.4 (see Fig. 8). The 1.25 μm reflectance test is applied only to potential cloudy pixels that have passed previous tests.

H. Ice Discrimination

To further discriminate ice surfaces from water clouds, pixels that have reflectance values at 1.37 μm greater than 0.1 are assumed to be ice surfaces and eliminated from consideration as cloudy. Referring to Fig. 8, it can be seen that for water clouds and bright snow-covered surfaces, reflectance values at 1.37 μm are quite low, much less than

0.1. Ice surfaces, however, display a significant reflectance signal at this wavelength

6. ALOGRITHM APPLICATIONS

The cloud cover detection process defined in Fig. 6 has been applied to a set of 20 Hyperion scenes with varying cloud cover and type, surface characteristics and seasonal collection times. The cloud cover detection algorithm was applied independently to each pixel in a scene; effects from adjacent pixels did not influence the computations. The primary output product was line-by-line statistics of the presence of cloud-free pixels, water-cloud, and ice-cloud covered pixels. Examples of the Hyperion scenes that were used in the testing are shown in figure 1. An RGB rendition of the scene is shown along with the computed cloud mask. For each of the cases shown in figure 1 and figure 9, the associated figure depicting the cloud cover uses the following color scheme: blue – cloud-free, gray/maroon – low/mid cloud, orange – mid/high cloud.

Kokee Hawaii:

This scene was collected on May 22, 2002 at 2056 UTC over the island of Kauai, HI. The scene is characterized by partly cloudy conditions with cumulus clouds present over land and water (Fig. 1). Clear regions are also visible. The algorithm does well detecting clouds over the land; over the water the main cloud region is masked but some areas of thin cloud cover may not be identified. The routine seems to miss a small amount of cloud cover over land, mostly cloud edges, which would support a slight reduction in the threshold value for the reflectance test.

Cheyenne Wyoming:

This scene was collected on March 5, 2002 at 1720 UTC near Cheyenne, WY. The scene is characterized by partly cloudy conditions with high thin clouds overlying snow-covered hilly terrain (Fig. 9). The algorithm accurately identifies the bright snow-covered terrain as a surface feature with the possible exception of some areas near the edge of the high clouds. These areas seem to be shadowed either by the high clouds or self shadowed due to terrain variations and the moderate sun angle (36 degrees above the horizon)

7. SUMMARY

A validation for performing on-board cloud cover assessment and a technique for estimating the cloud amount in a hyperspectral scene have been described. The key objectives were to determine what performance was needed to do cloud assessment on-board an existing satellites due to limitations in performance of the present flight computers. The cloud assessment algorithm was designed to perform cloud cover detection onboard the EO-1 satellite, which has never been accomplished before. The technique required calibrated Level 1B radiances, which are converted to

reflectance values and processed through the cloud cover routine to produce a cloud mask for the observed image. The routine was tested on numerous Hyperion images collected over a wide range of surface and atmospheric conditions. Onboard testing of the algorithm was completed March 22, 2003. Key targeted future functionality is to use this cloud assessment to make alternate scene selection, i.e. if the cloud cover estimate is greater than desired for a particular scene, then a decision can be made to collect a different scene on the next orbital pass. This avoids the process of collecting, storing, transmitting to ground, and processing the scene only to find out that the scene is obscured by clouds and not usable.
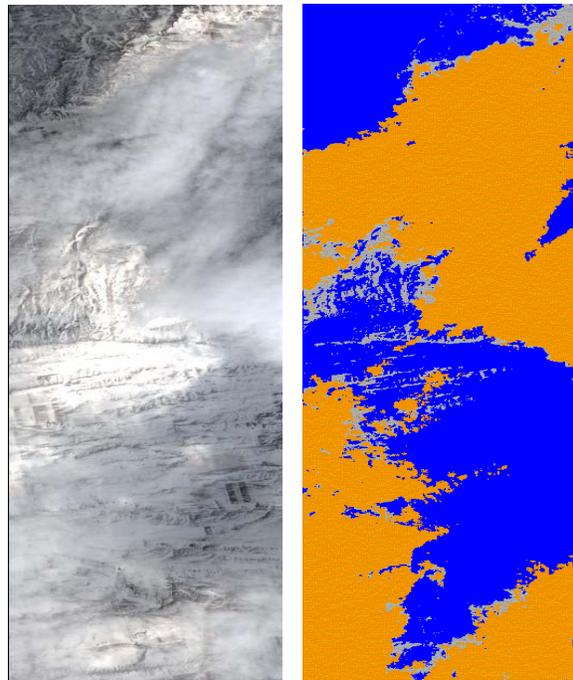
Fig 9. Hyperion image collected near Cheyenne, WY displaying partly cloudy conditions with high thin clouds over snow covered hilly terrain.

8. REFERENCES

[1] Ackerman, S.A., K.I. Strabala, W.P. Menzel, R.A. Frey, C.C. Moeller, and L.E. Gumley, "Discriminating clear sky from clouds with MODIS," *J. Geophy. Res.,* **103**, pp. 32141-32157, 1998.

[2] Pearlman, J., S. Carman, C. Segal, P. Jarecke, and P. Barry, "Overview of the Hyperion Imaging Spectrometer for the NASA EO-1 Mission," *Proceedings of IGARRS 2001,* Sydney, Australia, 2001.

[3] Berk, A, L.S. Bernstein, G.P. Anderson, P.K. Acharya, D.C. Robertson, J.H. Chetwynd, and S.M. Adler-Golden, "MODTRAN Cloud and Multiple Scattering Upgrades with Application to AVIRIS," *Remote Sens. Environ.,* **65**, pp. 367-375, 1998.

[4] Gao, B.-C and Y.J. Kaufman, "Correction of Thin Cirrus Effects in AVIRIS Images Using the Sensitive 1.375-μm Cirrus Detecting Channel*," Summaries of the Fifth Annual JPL Earth Science Workshop*, JPL Publication 95-4, pp. 59-62, Pasadena CA, 1995.

[5] Gao, B.-C, Y.J. Kaufman, W. Han, and W.J. Wiscombe, "Removal of Thin Cirrus Path Radiances in the 0.4 – 1.0-μm Spectral Region Using the 1.375-μm Strong Water Vapor Absorption Channel," *Summaries of the Seventh JPL Airborne Earth Science Workshop*, JPL Publication 97-21, pp. 121-130, Pasadena CA, 1998.

[6]   Tucker, C.J., "Red and Photographic Infrared Linear Combinations for Monitoring Vegetation," *Remote Sens. Environ.*, **8**, pp. 127-150, 1979.

9. TEAM MEMBERS

PI; Dan Mandl/GSFC
Co-I Jerry Miller/GSFC
Tom Brakke/GSFC
Michael Griffin/MIT-LL
Hsaio-hua Burke/MIT-LL
Carolyn Upshaw/MIT-LL
Kris Ferrar/MIT-LL
Stuart Frye/GSFC-Mitretek
Seth Shulman/GSFC-CSC
Robert Bote/GSFC-Honeywell
Joe Howard/GSFC-Honeywell
Jerry hengemihle/GSFC-Microtel
Bruce Trout/GSFC-Microtel
Scott Walling/GSFC-Microtel
Nick Hengemihle/GSFC-Microtel
Lawrence Ong/GSFC-SSAI
Larry Alexander/GSFC-Compaq